Phase transitions and the weak relaxor ferroelectric phase in $Ba_{7/8}(La_{0.5}Na_{0.5})_{1/8}TiO_3$

2002 J. Phys.: Condens. Matter 14 8445

(http://iopscience.iop.org/0953-8984/14/36/304)

INSTITUTE OF PHYSICS PUBLISHING JOURNAL OF PHYSICS: CONDENSED MATTER

J. Phys.: Condens. Matter **14** (2002) 8445–8454 PII: S0953-8984(02)38184-0

Phase transitions and the weak relaxor ferroelectric phase in $Ba_{7/8}(La_{0.5}Na_{0.5})_{1/8}TiO_3$

S Komine and E Iguchi[1]

Division of Materials Science and Engineering, Graduate School of Engineering, Yokohama National University, Tokiwadai, Hodogaya-Ku, Yokohama, 240-8501, Japan

E-mail: iguchi@post.me.ynu.ac.jp

Received 14 June 2002
Published 29 August 2002
Online at stacks.iop.org/JPhysCM/14/8445

Abstract

In order to elucidate the correlation between the phase transitions and presence of a relaxor phase in the composition $Ba_{1-x}(La_{0.5}Na_{0.5})_xTiO_3$, intermediate between $BaTiO_3$ and $(La_{0.5}Na_{0.5})TiO_3$, measurements of the dielectric permittivity in the temperature range 10–500 K in a heating–cooling cycle and powder x-ray diffraction measurements down to 150 K have been carried out on $Ba_{7/8}(La_{0.5}Na_{0.5})_{1/8}TiO_3$, which has three phase transitions and weak relaxor ferroelectric character below 500 K. The hysteresis observed in the dielectric permittivity in the heating–cooling cycle and a weak tetragonality deduced from the c/a ratio being very close to the cubic ratio for the tetragonal phase lead to the prediction of coexistence of multiple phases. The shrinkages of the temperature regions of the low-symmetry phases with increasing x in $Ba_{1-x}(La_{0.5}Na_{0.5})_xTiO_3$ confirm this prediction. The deformation mode changes gradually from Γ_{15} to R_{25} with increase of x. The relation between the deformation mode and the phase transitions is also discussed.

1. Introduction

Relaxor ferroelectrics were first described by Smolenskii *et al* [1] and have been investigated by many authors from the fundamental scientific and industrial applications points of view [2], owing to their interesting and important properties, such as a diffuse phase transition, frequency dependence of the dielectric permittivity and the large piezoelectricity at the morphotropic phase boundary (MPB) composition. At present, it is generally accepted that these features of relaxors correlate strongly with random potentials [3] and polar nanodomain structures [4–10].

Many relaxor ferroelectric compounds have modulated perovskite structures of the $A(B', B'')O_3$ type. In $A(B', B'')O_3$ systems, the B' and B'' cations have different electronic charges (($B' = Mg^{2+}$, $B'' = Nb^{5+}$), ($B' = Sc^{3+}$, $B'' = Ta^{5+}$) and so on [1, 11, 12]). The

[1] Author to whom any correspondence should be addressed.

combination of the charges at the B′ and B″ sites plays an important role in the dielectric character of relaxor ferroelectric materials, because the disordering of two kinds of B-site ion (B′ and B″) brings about polar nanodomain structure [13] and random potentials which characterize relaxors. However, in $A(B', B'')O_3$ systems, the A-site ion is generally Pb^{2+}, as in $PbMg_{1/3}Nb_{2/3}O_3$ (PMN) [1, 14]. This is a disadvantage from the environmental point of view. In our previous work [15], we have reported on a Pb-free relaxor ferroelectric system, i.e., $Ba_{1-x}(La_{0.5}Na_{0.5})_xTiO_3$. The dielectric character of this system is dependent on x: classical ferroelectric near $x = 0$, relaxor ferroelectric around $x = 3/8$ and quantum paraelectric near $x = 1$.

In $BaTiO_3$, one of the end-members of the $Ba_{1-x}(La_{0.5}Na_{0.5})_xTiO_3$ system ($x = 0$), a phase transition occurs from rhombohedral (C_{3v}) to cubic (O_h) through orthorhombic (C_{2v}) and tetragonal (C_{4v}) as temperature increases to about 400 K. Each transition is a first-order transition with softening of the Γ_{15} mode. $La_{0.5}Na_{0.5}TiO_3$, another end-member ($x = 1$), belongs to the $Ln_{0.5}Na_{0.5}TiO_3$ system (Ln stands for lanthanide), which is a quantum paraelectric and the deformation mode is R_{25} [16–18]. Itoh *et al* [19] elucidated the details of the relation between classical ferroelectrics and quantum paraelectrics. For the compound $Ba_{1-x}(La_{0.5}Na_{0.5})_xTiO_3$, intermediate between $BaTiO_3$ and $La_{0.5}Na_{0.5}TiO_3$, careful examination and consideration of the change of the deformation mode and dielectric properties are required, because each of the two end-members includes a different deformation mode.

The compound $Ba_{7/8}(La_{0.5}Na_{0.5})_{1/8}TiO_3$ ($x = 1/8$) is very close to $BaTiO_3$ as regards dielectric properties, as reported in our previous work [15]. This must be ascribed to the crystal structure being similar to that of $BaTiO_3$; as a result, $Ba_{7/8}(La_{0.5}Na_{0.5})_{1/8}TiO_3$ also shows a tetragonal–cubic transition. The Curie–Weiss relation indicates, however, that this transition in $Ba_{7/8}(La_{0.5}Na_{0.5})_{1/8}TiO_3$ is second order, while it is a first-order transition in $BaTiO_3$. Moreover, $Ba_{7/8}(La_{0.5}Na_{0.5})_{1/8}TiO_3$ exhibits relaxor ferroelectricity, although weakly.

It is, therefore, of great importance and interest to study the correlation between the dielectric properties and phase structures of this compound. In view of this, in the present work, we have investigated the details of the dielectric properties and the phase transitions in $Ba_{7/8}(La_{0.5}Na_{0.5})_{1/8}TiO_3$, and examined the possibility of a transformation from a classical ferroelectric to a relaxor ferroelectric via the annihilation of some phase transitions. Towards this end, the temperature dependences of the dielectric permittivity in both heating and cooling processes and powder XRD measurements below room temperature down to 150 K have been carried out. The results obtained experimentally have been considered, taking into account the deformation mode which is a very important factor in the relation between the relaxor behaviour and phase transitions in this system.

2. Experiment

The polycrystalline ceramic sample of $Ba_{7/8}(La_{0.5}Na_{0.5})_{1/8}TiO_3$ was prepared by a conventional solid-state synthesis technique. The starting materials were $BaCO_3$ (3N), La_2O_3 (4N), Na_2CO_3 (3N) and TiO_2 (3N). The mixture was calcined in pure oxygen at 1200 °C for 12 h. After calcining had been performed twice, pelletized samples were sintered in pure oxygen at 1350 °C for 5 h. Powder XRD measurements were executed at 150, 210, 230, 280 and 310 K in the heating process by using Cu Kα radiation (Mac Science Technology MXP18VAHF) generated at 40 kV, 300 mA. The sample for the measurements of the dielectric permittivity was rectangular with a surface area of 25 mm^2 and thickness of 1 mm. Both of the square faces were polished with diamond paste and then gold evaporated on to provide an electrode. The dielectric permittivities ε_r' and ε_r'' were measured as parametric functions of frequency in the temperature range 10–500 K in the heating–cooling cycle, at the rate

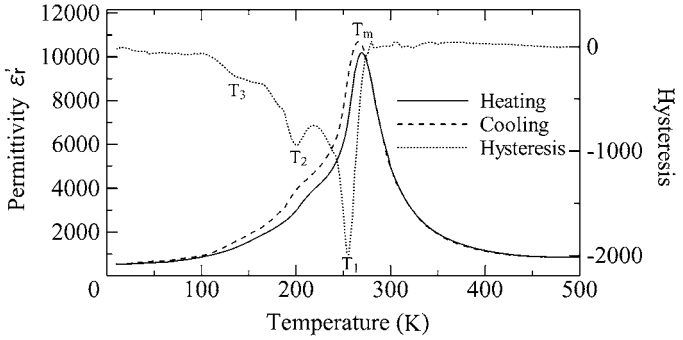

Figure 1. Temperature dependences of ε_r' in the heating–cooling cycle and the hysteresis $\varepsilon_r'(\text{heat}) - \varepsilon_r'(\text{cool})$ at 100 Hz.

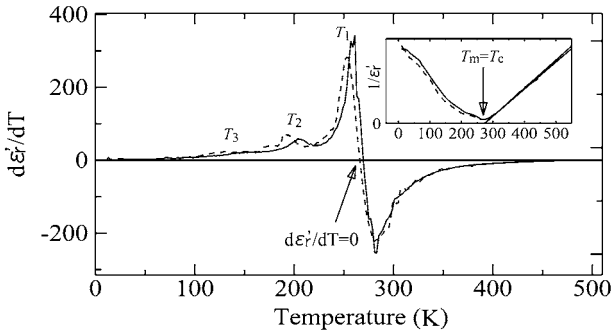

Figure 2. Temperature dependences of $\mathrm{d}\varepsilon_r'/\mathrm{d}T$ at 100 kHz. The solid curve represents the result in the heating process and the broken curve that in the cooling process. The inset shows the Curie–Weiss plots.

1 K min^{-1}, using an Agilent4294A precision impedance analyser. The dielectric permittivities were measured as functions of temperature, usually in 2 K increments but in 0.5 K increments around the phase transitions. Two thermocouples, copper–constantan pre-calibrated at 4.2, 77 and 273 K and alumel–chromel pre-calibrated at 77, 273 and 505 K (the melting point of tin, i.e., Sn) were employed so as to make the temperature measurements as accurate as possible. The range of frequency employed was 100 Hz–4 MHz.

3. Result

3.1. Phase transitions in $Ba_{7/8}(La_{0.5}Na_{0.5})_{1/8}TiO_3$

Figure 1 shows the temperature dependence of the dielectric permittivity in the heating–cooling cycle at 100 kHz. Furthermore, the hysteresis, which is defined as $\varepsilon_r'(\text{heating}) - \varepsilon_r'(\text{cooling})$, is also plotted against temperature. The temperature of the permittivity maximum T_m is about 270 K at 100 kHz. The hysteresis is clearly detectable below T_m, and there are three peaks, at T_1, T_2 and T_3. The hysteresis is not observable at very low and very high temperatures in the measurement temperature range.

In order to show the phase transitions clearly, $\mathrm{d}\varepsilon_r'/\mathrm{d}T$ is plotted against temperature in figure 2. The solid and broken curves correspond to the heating and cooling processes at 100 kHz. There are also four temperatures marked, corresponding to T_m, T_1, T_2 and T_3 in

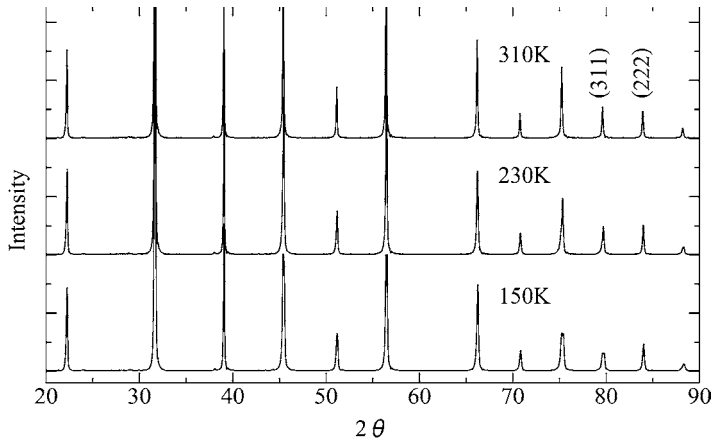

Figure 3. The XRD patterns of $Ba_{7/8}(La_{0.5}Na_{0.5})_{1/8}TiO_3$ at 150, 230 and 310 K.

figure 1. T_m was determined by using the relation $d\varepsilon'_r/dT = 0$, while T_1, T_2 and T_3 are the peak temperatures in the hysteresis below T_m in figure 1. The inset in figure 2 shows the Curie–Weiss plots, i.e., $1/\varepsilon'_r$ versus T. Thus the Curie temperature T_C is found to be equal to T_m. This is one of the characteristics peculiar to second-order phase transitions. The existence of the hysteresis is, however, indicative of a first-order phase transition. It is very strange that the prediction made on the basis of the hysteresis is not consistent with the prediction from the Curie–Weiss relation. $Ba_{7/8}(La_{0.5}Na_{0.5})_{1/8}TiO_3$ contains three phase transitions around T_1, T_2 and T_3. There must be some particularly strong relation between T_m and T_1, because T_1 is very close to T_m.

Figure 3 shows the XRD patterns of $Ba_{7/8}(La_{0.5}Na_{0.5})_{1/8}TiO_3$ at 150, 230 and 310 K, which include no impurity phases. The XRD results indicate that the crystal structure of this compound depends sensitively on temperature. The XRD results in figure 1 involve pseudo-cubic (311) and (222) reflections. Although there is only one peak due to the pseudo-cubic (311) reflection at 310 K, it splits into two or more peaks below 230 K. As for the pseudo-cubic (222) reflection, there is only one peak at 230 and at 310 K, but the FWHM (full width at half-maximum) at 230 K is larger than that at 310 K. The increase in FWHM may suggest the coexistence of multiple phases that have similar lattice parameters. In fact, the (222) reflection splits into multiple peaks at 150 K.

Figure 4 shows the variations of the lattice parameters (open squares) and the volume fraction (solid squares) with temperature. The vertical broken lines indicate the temperatures near the phase transitions, i.e., T_1 and T_2. The phase structure is: cubic at $T > T_1$; tetragonal between T_1 and T_2; and orthorhombic at $T < T_2$. The discontinuity in the lattice parameters and the volume fraction takes place at T_1. The tetragonal–cubic transition is then first order, not second order as predicted from the Curie–Weiss relation. $Ba_{7/8}(La_{0.5}Na_{0.5})_{1/8}TiO_3$ exhibits phase transitions similar to those of $BaTiO_3$, but the tetragonal parameter c/a ratio is very close to 1. The ratio is 1.0028 at 210 K and 1.0025 at 230 K, whereas it is 1.0110 at 300 K for $BaTiO_3$ (JCPDS code 05-0626).

3.2. Relaxor ferroelectrics

Figures 5(a) and (b) show the temperature dependences of the real and imaginary dielectric permittivity, ε'_r and ε''_r, as parametric functions of the applied field. The solid curves and

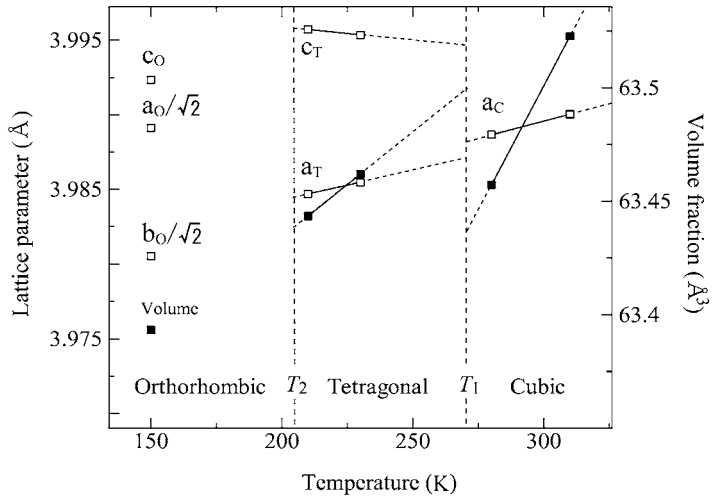

Figure 4. Lattice parameters (open squares) and volume fraction (solid squares) against temperature. All of lattice parameters are normalized to the perovskite structure.

broken curves indicate the results in the heating and cooling processes, as in figures 1 and 2. The dielectric permittivity in the cooling process is larger than that in the heating process. As the applied frequency increases, the real permittivity decreases, while the imaginary permittivity increases. At $T < T_m$, frequency dispersion takes place, particularly around the phase transition temperatures. It is interesting that the behaviour of ε_r'' around T_2 is quite different from that of ε_r'.

Figure 6 plots the dielectric permittivity against the applied frequency at various temperatures. The inset shows the temperature dependence of $\Delta\varepsilon_r'$, where $\Delta\varepsilon_r' = [\varepsilon_r'(100\text{ Hz}) - \varepsilon_r'(100\text{ kHz})]/\varepsilon_r'(100\text{ Hz})$, which is one of the measures characterizing the relaxor ferroelectric. At each temperature, the permittivity falls drastically when the applied frequency increases in the high-frequency region above 1 MHz. Below 10^5 Hz, the permittivity is nearly independent of the applied frequency at $T > 300$ K, but decreases gradually with increase of the applied frequency at $T < 250$ K. Since there are three minima, at T_1, T_2 and T_3, in the temperature dependence of $\Delta\varepsilon_r'$, there must be a strong correlation between the relaxor ferroelectric behaviour and the phase transitions. We denote the shift of T_m as $\Delta T_m = T_m(100\text{ kHz}) - T_m(100\text{ Hz})$; then $\Delta T_m \cong 0.5$ K for this compound. Although the magnitude of ΔT_m is small, the present experimental system guarantees that this result is valid for the following reasons. The same experiment has been carried out on $BaTiO_3$ and T_m is found to be independent of the applied frequencies, i.e., $\Delta T_m \cong 0$ K. Furthermore, the temperature changes during the measurements of the dielectric permittivities at several different applied frequencies are negligibly small at each temperature because they are measured within 5 s whereas the heating and cooling rate is 1 K min^{-1}. Since $\Delta T_m \neq 0$ for relaxor ferroelectrics, experimental estimation of the value of ΔT_m is also important for identifying relaxor ferroelectrics.

It is well known that the relaxor behaviour obeys the Vögel–Fulcher relation [20], i.e., $f = f_0\exp[-E_a/(T_m - T_{vf})]$, where f is the applied frequency and f_0, E_a and T_{vf} are phenomenological parameters. As shown in figure 7, $Ba_{7/8}(La_{0.5}Na_{0.5})_{1/8}TiO_3$ follows the Vögel–Fulcher relation with $f_0 = 1.4 \times 10^7$ Hz, $E_a = 3.5$ K and $T_{vf} = 268.8$ K.

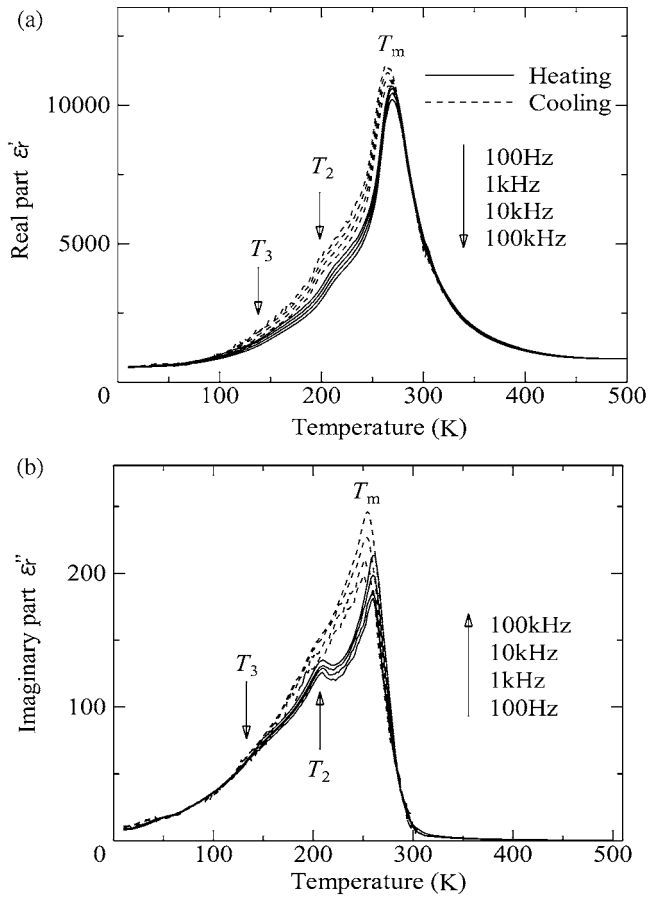

Figure 5. Temperature and frequency dependences of ε_r' (a) and ε_r'' (b) in the frequency range 100 Hz–100 kHz in the heating–cooling cycle.

4. Discussion

The experimental results of the dielectric permittivity and powder XRD investigations indicate that $Ba_{7/8}(La_{0.5}Na_{0.5})_{1/8}TiO_3$ contains three phase transitions at $T > 150$ K just like $BaTiO_3$ [21–23]: cubic (O_h) at $T > T_1$; tetragonal (C_{4v}) between T_1 and T_2; and orthorhombic (C_{2v}) at $T < T_2$. Although there is another transition temperature, T_3 (132 K), in the dielectric measurements, as shown in figures 1 and 6, there is no XRD evidence for this transition temperature because the XRD measurements were carried out above 150 K. By analogy with $BaTiO_3$, the rhombohedral phase (C_{3v}) may be expected at $T < T_3$ in $Ba_{7/8}(La_{0.5}Na_{0.5})_{1/8}TiO_3$. In comparison with the case of $BaTiO_3$, however, every transition temperature is lower and the temperature region of each phase is narrower for this compound. One example is the tetragonal phase which occurs in the range ~278–406 K (the temperature region is approximately 130 K) in $BaTiO_3$ [21, 23], but in the range ~200 K (T_2) to ~260 K (T_1) (the temperature region is about 60 K) in $Ba_{7/8}(La_{0.5}Na_{0.5})_{1/8}TiO_3$. This means that an increase of x in $Ba_{1-x}(La_{0.5}Na_{0.5})_xTiO_3$ (i.e., the amount of $La_{0.5}Na_{0.5}$ substituted for Ba^{2+}) narrows the temperature region of the tetragonal phase. In fact, the number of phase transitions was found to decrease from three to one with increase of x in our previous research [15] and $(La_{0.5}Na_{0.5})TiO_3$ ($x = 1$) does not exhibit the tetragonal phase [16, 24].

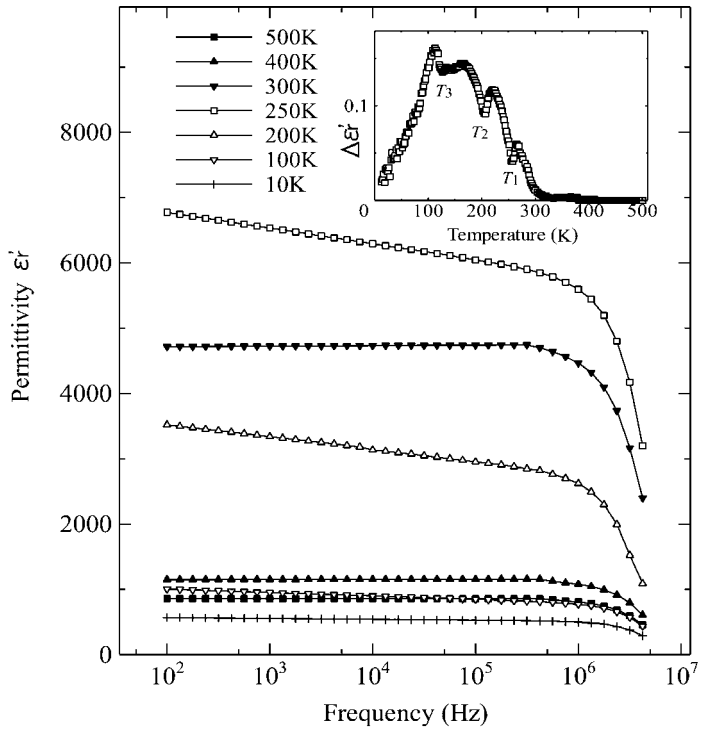

Figure 6. Frequency dependences of ε'_r at various temperatures. The temperature dependence of $\Delta\varepsilon'_r$ is plotted in the inset, where $\Delta\varepsilon'_r = [\varepsilon'_r(100\text{ Hz}) - \varepsilon'_r(100\text{ kHz})]/\varepsilon'_r(100\text{ Hz})$.

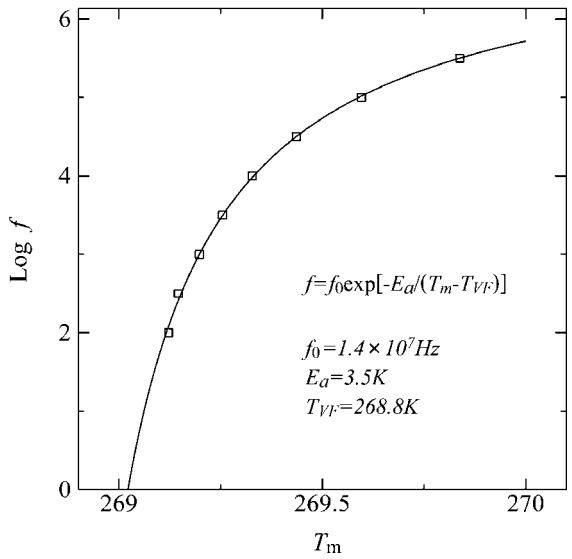

Figure 7. log f versus T_m: experimental plots (open squares) and the theoretical curve of the Vögel–Fulcher relation obtained by the curve-fitting method with the phenomenological parameters $f_0 = 1.4 \times 10^7$ Hz, $E_a = 3.5$ K and $T_{vf} = 268.8$ K.

It seems possible to explain such decay and annihilation of the tetragonal phase with increase of x in $Ba_{1-x}(La_{0.5}Na_{0.5})_xTiO_3$ by appealing to the hysteresis observed in $Ba_{7/8}(La_{0.5}Na_{0.5})_{1/8}TiO_3$ as follows. As shown in figure 1, the hysteresis is observable except in the temperature ranges above T_m and below $\sim$100 K. This indicates that the first-order phase transition proceeds gradually in the temperature region where the hysteresis takes place, implying that multiple phases coexist in this temperature region. In fact, the coexistences of multiple phases are guaranteed by the double hysteresis loops in $BaTiO_3$ around the phase transitions [25]. In a transition from a structure with a high point symmetry to a low-symmetry structure, furthermore, small differences in lattice parameters are required so as to suppress the increase in the lattice energy, which is crucial to the stabilization of a compound. When a cubic phase and a tetragonal phase coexist, there is also incoherency around boundaries between these phases, yielding strain fields. These restrictions require the lattice parameters of cubic and tetragonal phases to be very close in value to each other. In comparison with the case for $BaTiO_3$, the lattice parameters in the tetragonal phase are very close in value to the cubic parameters of $Ba_{7/8}(La_{0.5}Na_{0.5})_{1/8}TiO_3$. Such points strongly favour coexistence of multiple phases in this compound.

In $Ba_{1-x}(La_{0.5}Na_{0.5})_xTiO_3$, the deformation mode is the Γ_{15} mode at $x = 0$ and the R_{25} mode at $x = 1$, implying a change in soft mode with x. Since the c/a ratio in the tetragonal phase of this compound deviates very slightly from $c/a = 1$ (cubic), as detailed before, a rather weak tetragonality is introduced in practice. This tetragonality splits the threefold degeneracy of Γ_{15} in a cubic structure into a doublet and a singlet. In a case exhibiting weak tetragonality, such as $Ba_{7/8}(La_{0.5}Na_{0.5})_{1/8}TiO_3$, the splitting is small. These points also suggest the possibility of the coexistence of multiple phases.

If a phase transition occurs at Γ point ($|\vec{k}| = 0$), multiple phases cannot coexist because $\lambda = \infty$, where λ is the phonon wavelength. The coexistence of multiple phases requires the deviation of $\vec{k}$ from the Γ point, implying that phonons with short wavelengths are necessary. In order to resolve the threefold degeneracy of the Γ mode, on the other hand, phonons with wavelengths larger than a critical value are necessary. There is an argument that the deformation mode in $(La_{0.5}Na_{0.5})TiO_3$ ($x = 1$) is R_{25} [16]. There is then some $\vec{k}$-region in which the tetragonal phase stabilizes, and increase in x from 0 decreases phonon wavelengths. As a result, the deformation mode changes gradually from Γ_{15} to R_{25} with increase in x. Therefore, multiple phases coexist and the number of phase transitions decreases in the composition intermediate between $BaTiO_3$ and $(La_{0.5}Na_{0.5})TiO_3$, i.e., $Ba_{1-x}(La_{0.5}Na_{0.5})_xTiO_3$.

The ionic mass of the Na^+ ion is expected to play an important role in the phase transitions in this compound by analogy with $(Na_{1-x}K_x)_{0.5}Bi_{0.5}TiO_3$, in which light Na^+ ions frequently scatter phonons [26]. Furthermore, it is also noteworthy that the temperatures yielding the minima in the $\Delta\varepsilon_r'$–T relation of figure 6 are nearly equal to the temperatures at which the hysteresis in figure 1 has maxima for $Ba_{7/8}(La_{0.5}Na_{0.5})_{1/8}TiO_3$. This indicates that the dielectric hysteresis and the emergence of relaxor behaviour in this compound occur for the same reasons. It is well known that the coexistence of two phases enhances the relaxor ferroelectric character at the MPB composition [27, 28]. In $Ba_{7/8}(La_{0.5}Na_{0.5})_{1/8}TiO_3$, with its dielectric hysteresis and coexistence of multiple phases, a similar speculation regarding the MPB composition must arise.

The highest-symmetry structure in $Ba_{7/8}(La_{0.5}Na_{0.5})_{1/8}TiO_3$ is cubic and the crystallographic point group is O_h without spontaneous polarization. The point groups of the lower-symmetry structures, orthorhombic, rhombohedral and tetragonal, are C_{2v}, C_{3v} and C_{4v}. Although these structures involve spontaneous polarizations, the polarization axes in these low-symmetry structures are different from each other. Consequently, the coexistence of multiple phases with different polarization axes must yield a random potential in a crystal. There is a

possibility that the random potential induced in this way is related directly to the formation of nanodomain structures.

The speculation discussed above suggests that a hysteresis obtained in the similar way to that in the present study and the character of the relaxor ferroelectric are very important factors, which account chiefly for the coexistence of multiple phases and the change of the deformation mode in the $Ba_{1-x}(La_{0.5}Na_{0.5})_xTiO_3$ system, although there may be other relevant factors. More detailed elucidation of relaxor ferroelectric behaviour requires other experimental techniques such as the direct observation of multiple phases by TEM and the observation of Ti–O bond states by XPS and Raman spectroscopy. They will provide significant knowledge and are currently under way.

5. Conclusions

In order to elucidate the relationship of the phase transitions and relaxor behaviour in the composition $Ba_{1-x}(La_{0.5}Na_{0.5})_xTiO_3$, intermediate between $BaTiO_3$ ($x = 0$) and $(La_{0.5}Na_{0.5})TiO_3$ ($x = 1$), measurements of the dielectric permittivity in the temperature range 10–500 K in the heating–cooling cycle and powder XRD measurements down to 150 K have been carried out on $Ba_{7/8}(La_{0.5}Na_{0.5})_{1/8}TiO_3$, which has three phase transition points; every phase between transition points has a structure very similar to those of $BaTiO_3$. Although $Ba_{7/8}(La_{0.5}Na_{0.5})_{1/8}TiO_3$ also exhibits dielectric behaviour similar to that of $BaTiO_3$, this compound presents several significant differences from $BaTiO_3$, i.e., the second-order transition deduced from the Curie–Weiss relation, the long-range hysteresis in the dielectric permittivity in the heating–cooling cycle, the lowering of every transition temperature, the narrow temperature regions of the low-symmetry phases and the emergence of weak relaxor behaviour.

The deformation mode changes gradually from Γ_{15} to R_{25} with increase of x in $Ba_{1-x}(La_{0.5}Na_{0.5})_xTiO_3$, which is associated with the variation in the phonon wavelengths. There is a high possibility that such features of $Ba_{7/8}(La_{0.5}Na_{0.5})_{1/8}TiO_3$, different from those of $BaTiO_3$, as described above, are ascribable to change in the phonon wavelengths from that at the Γ point in the cubic structure. Light Na^+ ions frequently scattering phonons also assist in shortening the effective phonon wavelengths. The weak tetragonality in this compound, with the c/a ratio deviating slightly from the cubic one, is also indicative of shorter wavelengths compared with those of $BaTiO_3$. Such short wavelengths lead to the coexistence of multiple phases, which give rise to the emergence of relaxor behaviour in $Ba_{7/8}(La_{0.5}Na_{0.5})_{1/8}TiO_3$.

Acknowledgments

The authors are indebted to Dr F Munakata for useful discussions of the work. This work was supported by a Grant-in-Aid for Science Research from the Ministry of Education, Science and Culture, Japan (No 11650716), and a scholarship from Seimi Chemical Co., Ltd. The XRD measurements were carried out at Nissan Arc, Ltd.

References

[1] Smolenskii G A 1970 *J. Phys. Soc. Japan Suppl.* **26** 28
[2] Cross L E 1987 *Ferroelectrics* **76** 241
[3] Glinchuk M D and Farhi R 1996 *J. Phys.: Condens. Matter* **8** 6985
[4] Yao X, Chen Z L and Cross L E 1984 *J. Appl. Phys.* **54** 3399
[5] Viehland D, Jang S J, Cross L E and Wuttig M 1990 *J. Appl. Phys.* **68** 847

[6] Westphal V, Kleemann W and Glinchuk M D 1992 *Phys. Rev. Lett.* **68** 847
[7] Bursill L A and Lin P J 1986 *Phil. Mag.* B **54** 157
[8] Huang W H and Viehland D 1995 *Phil. Mag.* A **71** 219
[9] Yoshida M, Mori S, Yamamoto N, Uesu Y and Kiat J M 1998 *J. Korean Phys. Soc.* **32** S993
[10] Dkhil B, Kiat J M, Calvarin G, Baldinozzi G, Vakhrushev S B and Suard E 2001 *Phys. Rev.* B **65** 024104
[11] Malibert C, Kiat J M, Durand D, Bérar J F and Spasojevic-de Biré A 1997 *J. Phys.: Condens. Matter* **9** 7485
[12] Chu F, Setter N and Tagantsev A K 1993 *J. Appl. Phys.* **77** 5129
[13] Bokov A A and Ye Z G 2002 *Phys. Rev.* B **65** 144112
[14] Isupov V A 1989 *Ferroelectrics* **90** 113
[15] Komine S and Iguchi E 2002 *J. Phys.: Condens. Matter* **14** 2043
[16] Sun P H, Nakamura T, Shan Y J, Inaguma Y and Itoh M 1997 *Ferroelectrics* **200** 93
[17] Shan Y J, Nakamura T, Inaguma Y and Itoh M 1998 *Solid State Ion.* **108** 123
[18] Nakamura T, Shan Y J, Sun P H, Inaguma Y and Itoh M 1998 *Ferroelectrics* **219** 71
[19] Kasahara M, Hasebe H, Wang R, Itoh M and Yagi Y 2001 *J. Phys. Soc. Japan* **70** 648
[20] Viehland D, Jang S J, Cross L E and Wuttig M 1992 *Phys. Rev.* B **46** 8003
[21] Wemple S H, DiDomenico M Jr and Camlibel I 1968 *J. Phys. Chem. Solids* **29** 1797
[22] Merz W J 1949 *Phys. Rev.* **76** 1221
[23] Subarao E C 1973 *Ferroelectrics* **5** 267
[24] Inaguma Y, Shon J H, Kim I S, Itoh M and Nakamura T 1992 *J. Phys. Soc. Japan* **61** 3831
[25] Merz W J 1953 *Phys. Rev.* **91** 513
[26] Kreisel J, Glazer A M, Jones G, Thomas P A, Abello L and Lucazeau G 2000 *J. Phys.: Condens. Matter* **12** 3267
[27] Boutarfaia A 2001 *Ceram. Int.* **27** 91
[28] Zhu W Z, Yan M, Kholkin A L, Mantas P Q and Baptista J L 2002 *J. Eur. Ceram. Soc.* **22** 375